PUB-79-105 E-444
FERMILAB-PUB-79-105-E EFI 79-7
RECEIVED E-444
FEB 5 1979
DIRECTORS OFFICE
FERMILAB

# Comparison of Muon Pair Production to the Quark-Antiquark Annihilation Model

G. E. Hogan, K. J. Anderson, R. N. Coleman,[a] K. P. Karhi,
K. T. McDonald, C. B. Newman, J. E. Pilcher, E. I. Rosenberg,
G. H. Sanders,[b] A.J.S. Smith, and J. J. Thaler

Enrico Fermi Institute, University of Chicago, Chicago, Illinois 60637and

University of Illinois, Urbana, Illinois 61801 and

Joseph Henry Laboratories, Princeton University, Princeton, New Jersey 08540

## ABSTRACT

New data on muon pair production at 225 GeV/c by $\pi^-$, $\pi^+$ and proton beams are analyzed with regard to the production mechanism. The observed spin alignment of the pair and the dependence of the cross section on beam particle type are strong indications that the production is through electromagnetic quark-antiquark annihilation.

The preceding Letter[1] discussed the general features of production of high mass μ-pairs by 225 GeV/c beams of $\pi^-$, $\pi^+$, and protons on C, Cu, and W targets. In this article we discuss aspects of the data in the context of a theoretical framework.

The general formalism of lepton pair production by hadrons via a virtual intermediate photon has been discussed in the literature.[2] An important special case is the description in terms of quark-antiquark annihilation, first proposed by Drell and Yan and further developed by other authors.[3] The μ-pair production cross section for interacting hadrons A and B, neglecting $p_T$ and including three colors is:

$$\frac{d\sigma^2}{dMdx_F} = \frac{8\pi\alpha^2}{9M^3} \sum_i \frac{e_i^2}{(x_1+x_2)} \left[ x_1 f_i^A(x_1) x_2 f_{\bar{i}}^B(x_2) + x_1 f_{\bar{i}}^A(x_1) x_2 f_i^B(x_2) \right] \quad (1)$$

where $x_{\substack{1\\2}} = (\pm x_F + \sqrt{x_F^2 + 4M^2/s})/2$ are the momentum fractions (Feynman-x) of the annihilating quarks in the projectile and target hadrons,

$xf_i^A(x)$ is the momentum spectrum for quarks of flavor i in hadron A.

$x_F \equiv 2P_L^*/\sqrt{s}$ in this analysis where $P_L^*$ is the μ-pair longitudinal momentum in the overall center of mass.

Thus, the observed mass and Feynman-x ($x_F$) spectra for the data reflect the distributions of the annihilating quarks.

This mechanism predicts striking differences for the lepton pair production cross section in nucleon-nucleon scattering compared to pion-nucleon scattering. In the nucleon-nucleon case the interacting particles contain no valence antiquarks and only antiquarks from the $q\bar{q}$ sea can contribute. Since the probability density functions for the sea quarks fall steeply with $x_1$ and $x_2$ the observed mass spectrum should fall rapidly with mass for fixed $x_F$.

Incident pions, on the other hand, contain a valence antiquark which has a significant probability of being found at large $x_1$. Thus, the cross section for pion induced pairs should fall more slowly with mass than for incident protons.

To permit comparison of $\pi^-$ and proton induced cross sections at the highest possible mass values, we have used the proton results of Yoh et al.[4] The cross section ratio is shown in Fig. 1, The $\pi^-$ to proton cross section ratio rises to over 100 at a mass of 10 GeV/$c^2$ in dramatic agreement with expectations.

Consider next the comparison of the $\pi^+$ and $\pi^-$-induced $\mu$-pair production cross sections. In this case, valence quarks and antiquarks from the interacting particles should dominate production if $x_1$ and $x_2$ are both large. In this experiment a carbon target was used so that the target is exactly symmetric in u and d quark distributions ($u^p=d^n$, $d^p=u^n$). In the case of an incident $\pi^-$ the valence antiquark is a $\bar{u}$ with charge -2/3 while for an incident $\pi^+$ it is a $\bar{d}$ with charge 1/3. Since the pair production varies like the square of the quark charge, one expects $\sigma(\pi^+C\rightarrow\mu^+\mu^-...)/\sigma(\pi^-C\rightarrow\mu^+\mu^-...)$ to be 1/4. If $x_1$ and $x_2$ are not both large, sea antiquarks can contribute and the cross section ratio approaches 1 as $x_1$, $x_2$ approach 0. Figure 2a shows the measured $\pi^+/\pi^-$ cross section ratio as a function of pair mass for $x_F > 0$. It is seen to be near unity for the J/$\psi$ as might be expected for strong production from charge symmetric initial states. As the pair mass increases above 3.1 GeV/$c^2$ the ratio falls toward 1/4. Any deviation of the ratio from unity is indicative of an electromagnetic process and the limiting value of 1/4 is predicted by the $q\bar{q}$ annihilation mechanism.

The solid line in Fig. 2a is a calculation of the $\pi^+/\pi^-$ cross section ratio from the pion and nucleon structure functions together with the contribution of the observed resonances. The determination of the pion structure function is discussed in the following Letter. Since the $\pi^+$ and $\pi^-$ structure functions are the same, the approach to 1/4 is primarily dependent on the nucleon structure functions and in particular on the form of the nucleon sea quark distributions. Using the measured sea distributions of Kaplan et al.,[5] we find reasonable agreement with the data although these sea distributions have been determined only for $x_2 > 0.25$.

Figure 2b shows the $\pi^+/\pi^-$ ratio from this experiment as a function of $M/\sqrt{s}$ , together with other measurements.

Two variables, in addition to M, $x_F$ and $p_T$ are required to specify the μ-pair final state. Natural choices are the polar ($\theta^*$) and azimuthal angles of one of the muons in the μ-pair rest frame. The annihilation of two spin-1/2 fermions to a $1^-$ intermediate state should lead to a $1 + \cos^2\theta^*$ distribution where $\theta^*$ is measured from the $q\bar{q}$ direction in the μ-pair c.m. system. If the $p_T$ of the final state μ-pair is zero, the beam and target define the $q\bar{q}$ direction. If $p_T$ is non-zero, the $q\bar{q}$ direction is not determined. Collins and Soper[6] have suggested using the vector which bisects the angle between the beam and the reverse of the target vector as the best average estimate of the $q\bar{q}$ direction.

The distribution of the polar (helicity) angle has been examined for mass regions below the J/ψ ($2.0 < M < 2.7$ GeV/$c^2$), the J/ψ ($2.7 < M < 3.5$ GeV/$c^2$), and above the J/ψ ($M > 3.5$ GeV/c ). The distributions are shown in Fig. 3 with their best fits to the form $1 + \lambda \cos^2\theta^*$. Results of the fits are given in Table I. The continuum region above and below the J/ψ shows strong evidence of the expected spin alignment. The J/ψ data are consistent with a flat angular distribution. The mass dependence of these distributions reflects a clear change in the underlying production mechanism for the J/ψ compared with the continuum. Similar results for the continuum are also obtained using either the s, t, or u-channel reference directions for the helicity angle.

A number of attempts have been made to explain the broad $p_T$ spectra for the μ-pair in terms of QCD corrections to the Drell-Yan mechanism. The corrections are expected to be most significant at higher $p_T$ and may modify the helicity angular distribution. Figure 3 and Table I give the helicity angular distribution for transverse momenta above and below 1 GeV/c. Evidence for spin alignment and a value of λ consistent with 1.0 are seen in both $p_T$ intervals.

Equation (1) implies the scaling result that $M^3 d\sigma/dM$ is a function only of $M^2/s$. It should be noted that this is not an especially unique feature of the annihilation mechanism since such a result also follows from dimensional arguments and has been found to apply also to the production of some narrow resonances.[8] Nevertheless, it is a condition which should be satisfied by the data.

Figure 4a shows our $\pi^- N \to \mu^+\mu^- X$ data compared with measurements at lower energies. This scaling prediction is not well satisfied by currently available $\pi^-$ data. However, some caution should be exercised in interpreting this result. The mass region covered by the low energy experiments is below the J/ψ where non-scaling resonance or continuum production may contribute. In this lower mass region both $\langle p_T \rangle$ and the A-dependence are observed to vary with mass[1] while they do not for the mass region of this experiment.

As a consistency check Fig. 4b shows our proton induced cross sections in comparison with other measurements. They are in good agreement and scaling is reasonably well satisfied.

The annihilation model also predicts scaling in the ratio of the $\pi^+$ induced to $\pi^-$ induced μ-pair production cross sections. The data are shown in Fig. 2b. The ratio is consistent with being a function of $M^2/s$ only.

In conclusion, we have performed a number of new tests of the Drell-Yan annihilation mechanism. The observed spin alignment of the μ-pair and the strong dependence of the cross section on beam particle species are in striking agreement with the hypothesis that the production proceeds through an electromagnetic quark-antiquark annihilation.

This work was performed at the Fermi National Accelerator Laboratory and supported by the Department of Energy and National Science Foundation.

## REFERENCES

[a]Present address: University of Rochester, Rochester, NY 14627.

[b]Present address: Los Alamos Scientific Laboratory, Los Alamos, NM 87545.

[1]K. J. Anderson et al., (submitted to Phys. Rev. Lett.)

[2]R. C. Oakes, Nuovo Cimento 44A, 440 (1966); C. S. Lam and Wu-Ki Tung, Phys. Rev. D18, 2447 (1978).

[3]S. D. Drell and T. M. Yan, Phys. Rev. Lett. 25, 316 (1970) and Ann. Phys. 66, 578 (1971). For a recent discussion see the review of T. M. Yan, VIII International Symposium on Multiparticle Dynamics, Kaysersberg, France, June, 1977.

[4]J. K. Yoh et al., Phys. Rev. Lett. 41, 684 (1978).

[5]D. M. Kaplan et al., Phys. Rev. Lett. 40, 435 (1978); L. M. Lederman, XIX International Conference on High Energy Physics, Tokyo, Japan, 1978. Use of the alternative (non SU(3) symmetric) fit of the nucleon sea quark distribution functions does not significantly affect the results.

[6]J. C. Collins and D. E. Soper, Phys. Rev. D16, 2219 (1977).

[7]See, for example, E. L. Berger, New Results in High Energy Physics-1978 (Vanderbilt Conference) AIP (1978); F. Halzen and D. M. Scott, University of Wisconsin preprint COO-881-21 (1978).

[8]T. K. Gaisser et al., Phys. Rev. D15, 2572 (1977).

[9]J. Alspector et al., preprint submitted to XIX International Conference on High Energy Physics, Tokyo, Japan, 1978, BNL-OG 419, UR-659/COO-202.

[10]S. V. Golovkin et al., preprint submitted to XIX International Conference on High Energy Physics, Tokyo, Japan, 1978.

[11]M. J. Corden et al., Phys. Lett. 76B, 226 (1978).

[12]M. A. Abolins et al., preprint submitted to XIX International Conference on High Energy Physics, Tokyo, Japan, 1978.

[13] L. M. Lederman and B. G. Pope, Phys. Lett. 66B, 486 (1977).

[14] D. Antreasyan et al., Phys. Rev. Lett. 39, 906 (1977).

TABLE I. Helicity angular distribution fits.

| Data Interval | | Fit Results | | | |
|---|---|---|---|---|---|
| Mass ($GeV/c^2$) | $p_T$ (GeV/c) | Flat $\chi^2/DF$ | $1+\cos^2\theta^*$ $\chi^2/DF$ | $1+\lambda\cos^2\theta^*$ $\lambda$ | $\chi^2/DF$ |
| 2.0 - 2.6 | All | 79.7/9 | 25.6/9 | 1.14±.17 | 25.0/8 |
| $J/\psi$ | All | 7.0/9 | 212.0/9 | -0.10±.05 | 4.7/8 |
| >3.5 | All | 44.6/9 | 6.6/9 | 1.30±.23 | 4.7/8 |
| >3.5 | <1.0 | 31.6/9 | 12.6/9 | 1.17±.29 | 12.2/8 |
| >3.5 | >1.0 | 36.4/9 | 11.2/9 | 1.47±.39 | 8.8/8 |

Fig. 1 The ratio of $\pi^-$ induced to proton induced $\mu$-pair cross section at $y_{cm} = 0.2$ as a function of mass. Proton data at 225 GeV/c has been calculated from the scaling observed in 200, 300, and 400 GeV/c data of Ref. 4.

Fig. 2 (a) $R = \sigma(\pi^+ C \to \mu^+\mu^- X)/\sigma(\pi^- C \to \mu^+\mu^- X)$ versus $M_{\mu\mu}$ at 225 GeV/c. The solid curve is described in the text.

(b) R versus $M/\sqrt{s}$ for data at 225 GeV/c and 40 GeV/c (Cu target) for continuum pairs. The curve is the same as shown in (a) but with resonance production excluded.

Fig. 3 Helicity angular distributions in three different mass intervals. The $M > 3.5$ GeV/$c^2$ interval is also shown divided in two $p_T$ intervals. The Collins-Soper angle $(\theta^*)$ is defined in the text.

Fig. 4 $M^3 d\sigma/dM$ versus $M^2/s$, the scaling form of the cross section for (a) $\pi^- N \to \mu^+\mu^- X$ and (b) $pN \to \mu^+\mu^- X$. Data from Ref. 4 and 14 are converted from the measured $d^3\sigma/dMdy$ $(y=0)$ to $d\sigma/dM$ $(x>0)$ by using the antiquark functions reported by the authors of Ref. 5 together with valence quark distributions from deep inelastic lepton scattering. The resulting $x_F$ distributions agree well with the observed spectrum in this experiment.

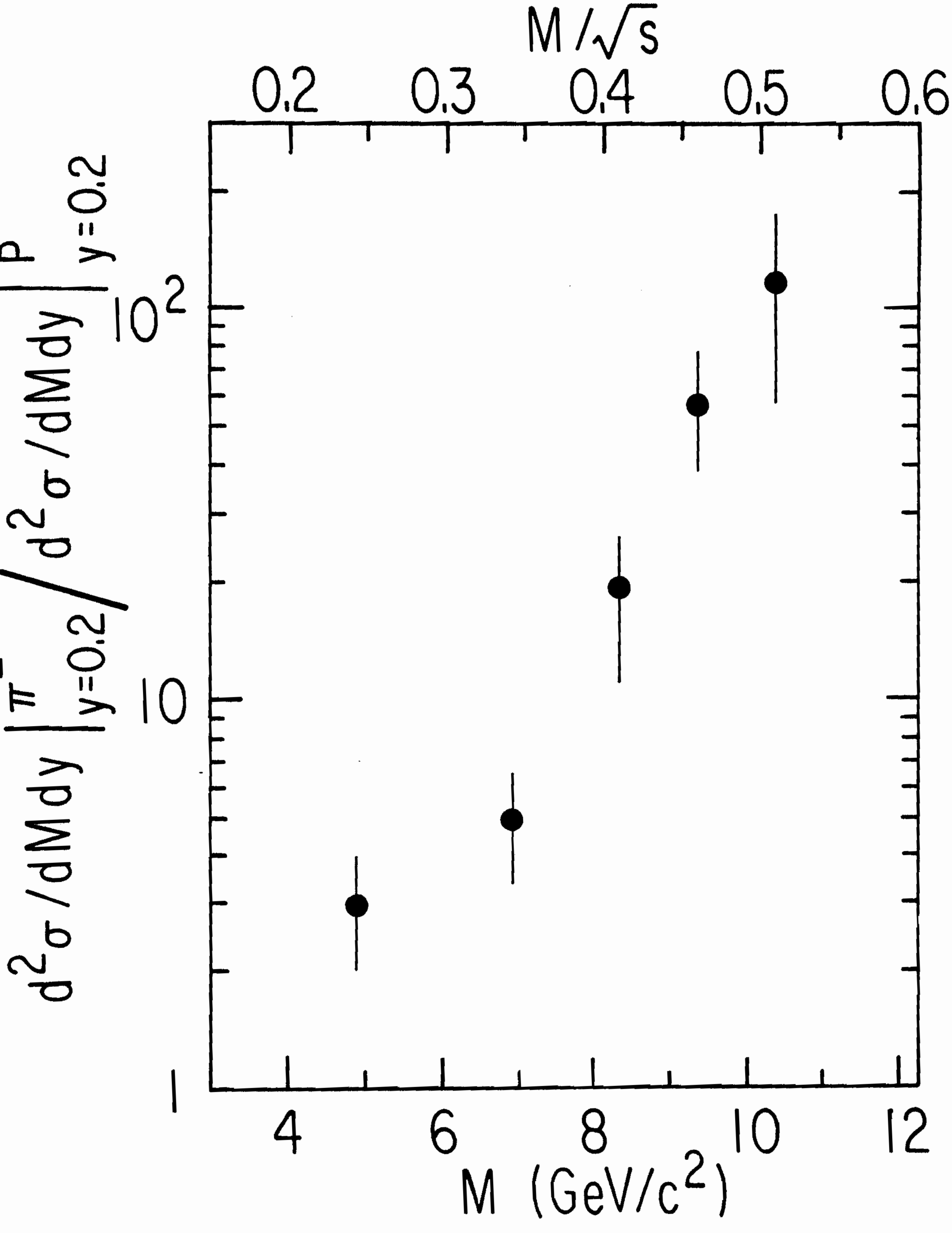

M/√s
0.2
0.3
0.4
0.5
0.6
d²σ/dMdy|π⁻ y=0.2 / d²σ/dMdy|P y=0.2
10²
10
1
4
6
8
10
12
M (GeV/c²)


Fig. 1

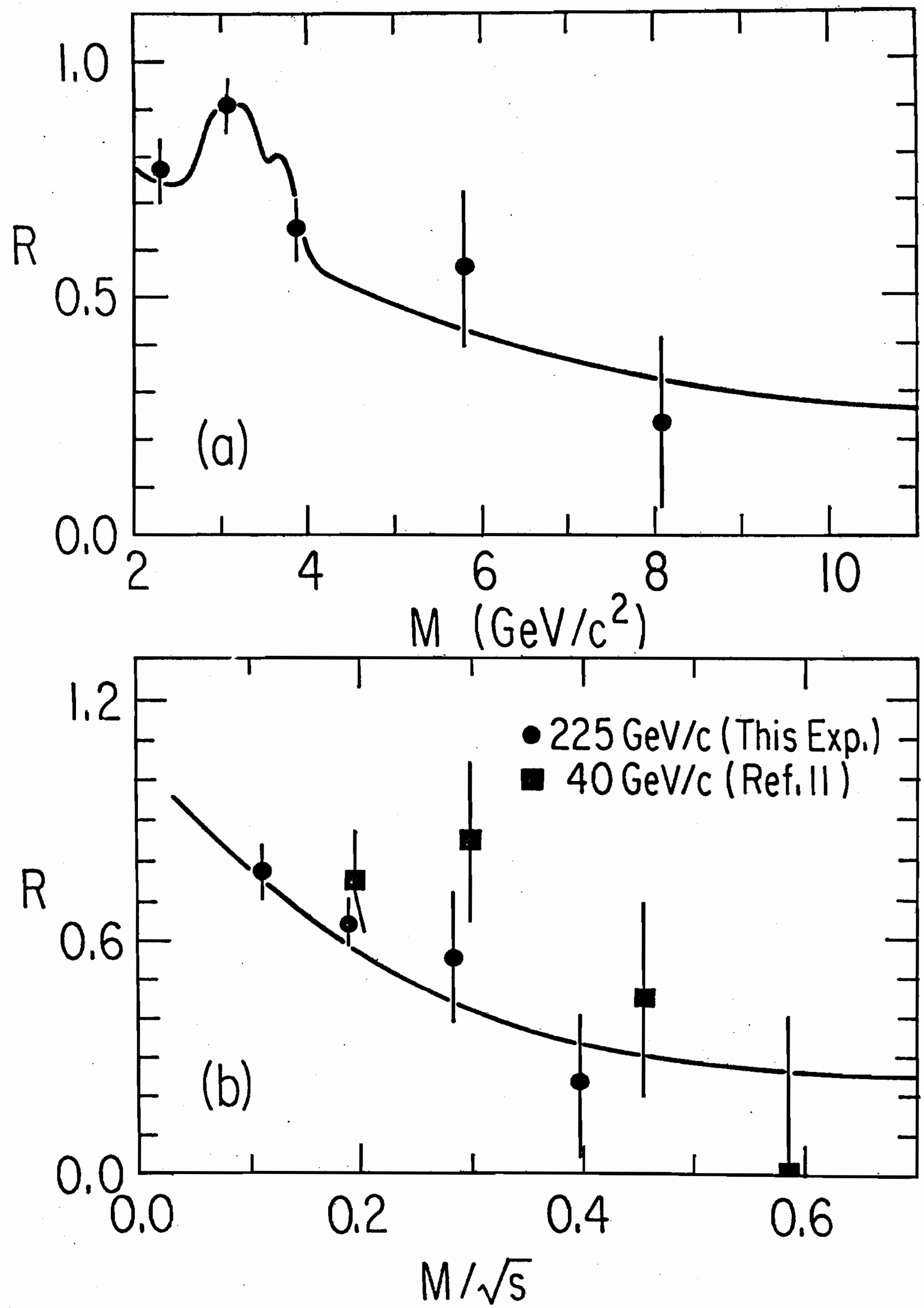

1.0
R
0.5
(a)
0.0
2
4
6
8
10
M (GeV/c²)
1.2
● 225 GeV/c (This Exp.)
■ 40 GeV/c (Ref. 11)
R
0.6
(b)
0.0
0.0
0.2
0.4
0.6
M/√s


Fig. 2

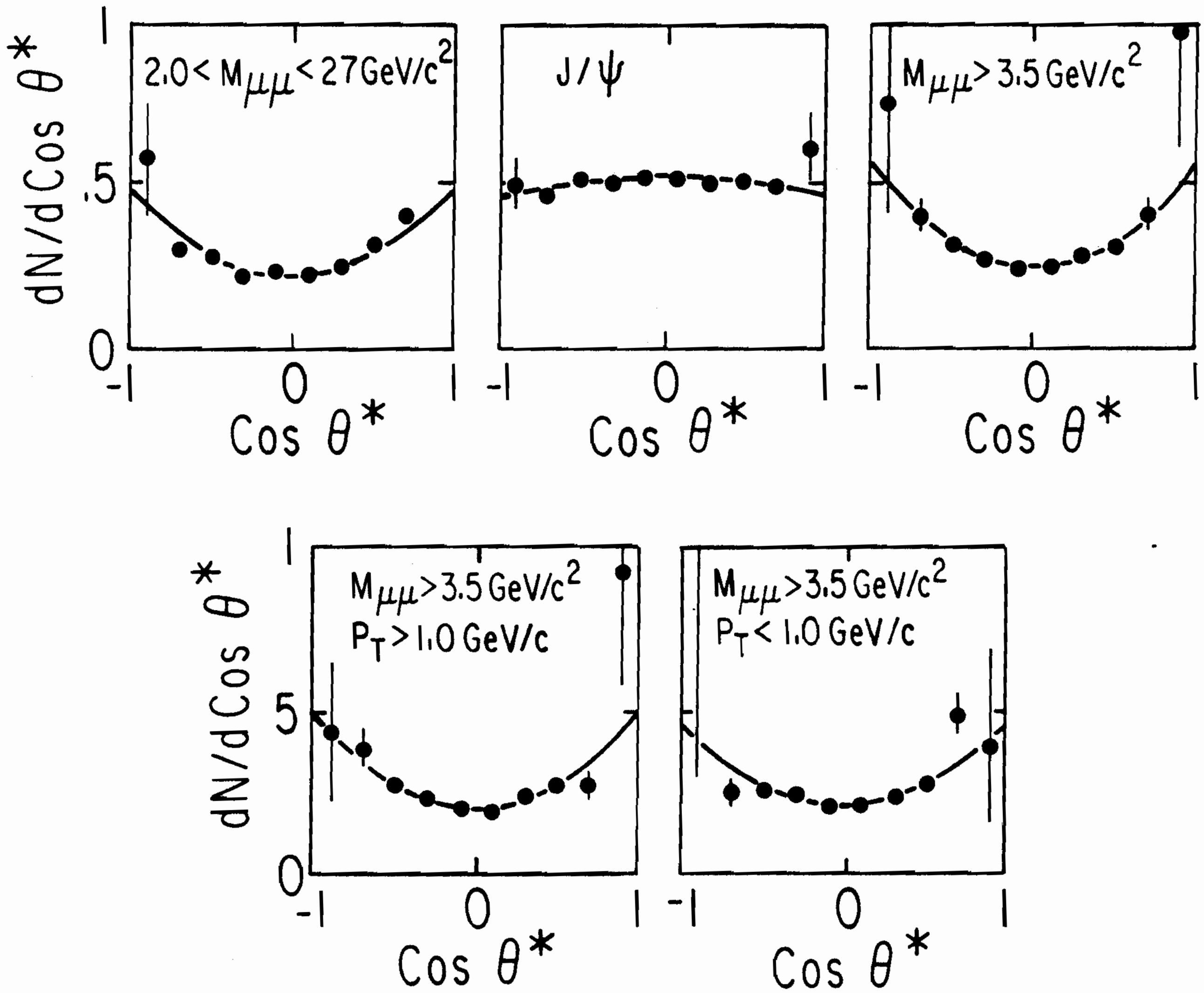

2.0 < Mμμ < 27 GeV/c²
J/ψ
Mμμ > 3.5 GeV/c²
Mμμ > 3.5 GeV/c²
PT > 1.0 GeV/c
Mμμ > 3.5 GeV/c²
PT < 1.0 GeV/c
dN/dCos θ*
Cos θ*


Fig. 3

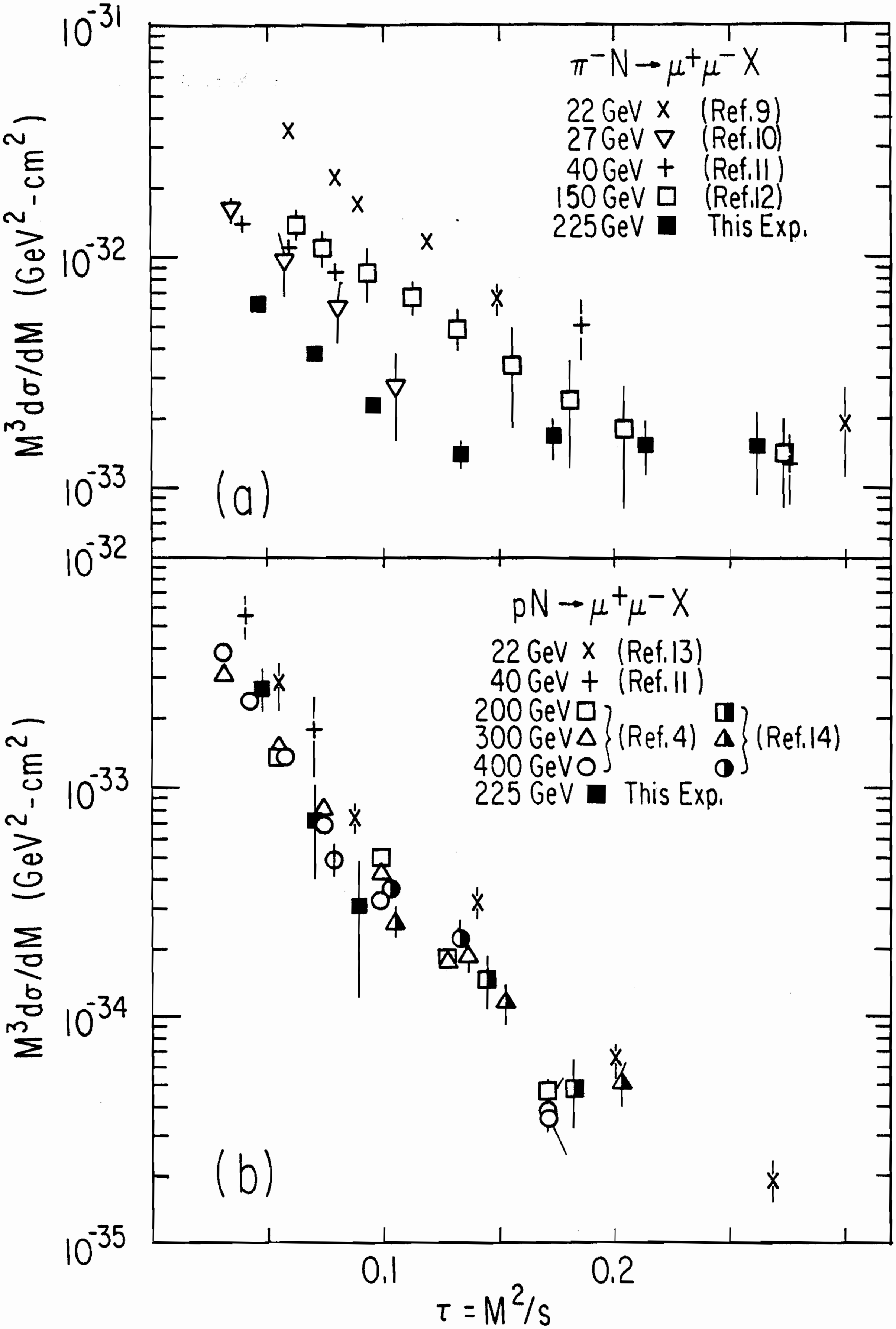

$10^{-31}$
$10^{-32}$
$10^{-33}$
$10^{-32}$
$10^{-33}$
$10^{-34}$
$10^{-35}$
$M^3 d\sigma/dM$ ($GeV^2$-$cm^2$)
$\pi^- N \to \mu^+ \mu^- X$
22 GeV x (Ref.9)
27 GeV ▽ (Ref.10)
40 GeV + (Ref.11)
150 GeV □ (Ref.12)
225 GeV ■ This Exp.
(a)
$pN \to \mu^+ \mu^- X$
22 GeV x (Ref.13)
40 GeV + (Ref.11)
200 GeV □
300 GeV △ (Ref.4)
400 GeV ○
(Ref.14)
225 GeV ■ This Exp.
(b)
0.1
0.2
$\tau = M^2/s$


Fig. 4